Supporting Information for:

Biodistribution of inhaled metal oxide nanoparticles at doses mimicking occupational exposure: a preliminary investigation using enhanced darkfield microscopy

Marissa Guttenberg;[1]‡ *Leonardo Bezerra;*[1]‡ *Nicole M. Neu-Baker;*[1] *María del Pilar Sosa Peña;*[1] *Alison Elder;*[2] *Günter Oberdörster;*[2] *Sara A. Brenner*[1*]

[1]State University of New York (SUNY) Polytechnic Institute, College of Nanoscale Science, Nanobioscience Constellation, Albany, New York, 12203, United States.

[2]University of Rochester, Department of Environmental Medicine 601 Elmwood Avenue, Rochester, New York, 14642, United States.

[*]**Corresponding author**
Sara A. Brenner, MD, MPH; State University of New York (SUNY) Polytechnic Institute, College of Nanoscale Science, Nanobioscience Constellation, 257 Fuller Road, Albany, New York, 12203, United States; sbrenner@sunypoly.edu; p: 518-956-7224; f: 518-437-8687.

Author Contributions
‡These authors contributed equally.

CHARACTERIZATION OF METAL OXIDE NANOPARTICLE SUSPENSIONS (Roth et al., 2015d)

Commercially available metal oxide nanoparticle suspensions used for semiconductor wafer polishing were used in this study. Three of the most common nanoparticle abrasives used in these aqueous slurries are silicon dioxide (SiO2; silica) aluminum oxide (Al_2O_3; alumina) and cerium (IV) oxide (CeO_2; ceria). The nanoparticles were characterized by scanning electron microscopy (SEM) with energy-dispersive x-ray spectroscopy (EDS), dynamic light scattering (DLS), single particle inductively coupled plasma-mass spectrometry (SP-ICP-MS), and scanning mobility particle sizing (SMPS).

Scanning electron microscopy (SEM) and energy-dispersive x-ray spectroscopy (EDS) (Roth et al., 2015d)

Samples were prepared for SEM onto a highly ordered pyrolytic graphite substrate mounted to stainless steel SEM stub by carbon tape. Imaging was conducted using a LEO 1550 SEM with a Schottky field emitter source at 5kV accelerating voltage, using a 30µm aperture, at a working distance of 3-6mm, with an InLens detector. Images obtained were analyzed manually to determine longest axial length and perpendicular axial length. SEM samples were analyzed by an EDS detector attachment for the LEO 1550 SEM at up to 20kV accelerating voltage, using a 60µm aperture, with a working distance of 15mm at a 15˚ take-off angle.

Dynamic light scattering (DLS) (Roth et al., 2015d)

Samples for DLS were diluted to approximately 100µg/mL. Size measurements were conducted by a Malvern Zetasizer system, assuming water properties for solvent parameters and taking 3 measurements with a minimum of 15 runs per measurement.

Single particle inductively coupled plasma-mass spectrometry (SP-ICP-MS) (Roth et al., 2015d)

SP-ICP-MS samples were prepared from slurries by dilution into HPLC water and were analyzed by PerkinElmer (Shelton, CT) using a Nexion 300 D SP-ICP-MS in single particle mode (final sample dilutions of 10^7-10^8). Assay of selected materials (silicon, aluminum, cerium) was conducted. The result was multiplied by a correction factor derived from mass-ratios contributed by the oxide component of the metal oxide with the assumption of stoichiometric ratios (SiO_2, Al_2O_3, CeO_2) to determine the concentrations of silica, alumina, and ceria (IV).

Scanning mobility particle sizing (Roth et al., 2015d)

Samples were prepared for SMPS by 1:99 dilution into buffer (20mM aqueous ammonium acetate at pH 8). Analysis was conducted by a TSI SMPS Model 3080 acting to electrostatically filter particles before detection by a TSI Condensation Particle Counter Model 3772. The SMPS was fed by a TSI Electrospray Aerosol Generator Model 3480 designed to deliver a constant 0.8L/min air flow with a known loss. This was combined with a known rate of 135s/scan, 103 size bins/scan, a known capillary pressure drop, and system temperature to determine a correction function for SMPS efficiency of particle counts.

Characterization Results (Roth et al., 2015d) Characterization results modified with permission from Sosa Peña et al. 2016 (Supplemental Information); copyright 2016 Wiley.

Table S1. Slurry nanoparticle diameter (modified from Roth et al., 2015d)

Sample	DLS (nm)	SEM[a] (nm) ± SD	SP-ICP-MS (nm)	SMPS (nm)
SiO_{x-3}	61.84	29.7 ± 6.8	114	100
AlO_{x-2}	100.1	20.3[b] ± 4.3	35	48
CeO_{x-1}	64.30	35.0 ± 15.4	28	65

[a]SEM diameter calculation was modeled on approximating particles as ellipses and normalizing to the diameter of a circle with equal area to the ellipse.
[b]Appeared as "N/A" in Roth et al. Diameter of 20.3nm was obtained after refinement of imaging techniques.

Refer to Roth et al., 2015d for a more in-depth comparison of characterization methods and a discussion of the strengths and limitations of each. Of the techniques compared by Roth et al., SEM was the most appropriate and accurate method for nanoparticle sizing since other methods (DLS, SP-ICP-MS, and SMPS) likely also size aggregates and agglomerates in addition to single particles. This uncertainty is due to the absence of a direct visualization component in those techniques.

Figure S1: SEM images of metal oxide nanoparticles.

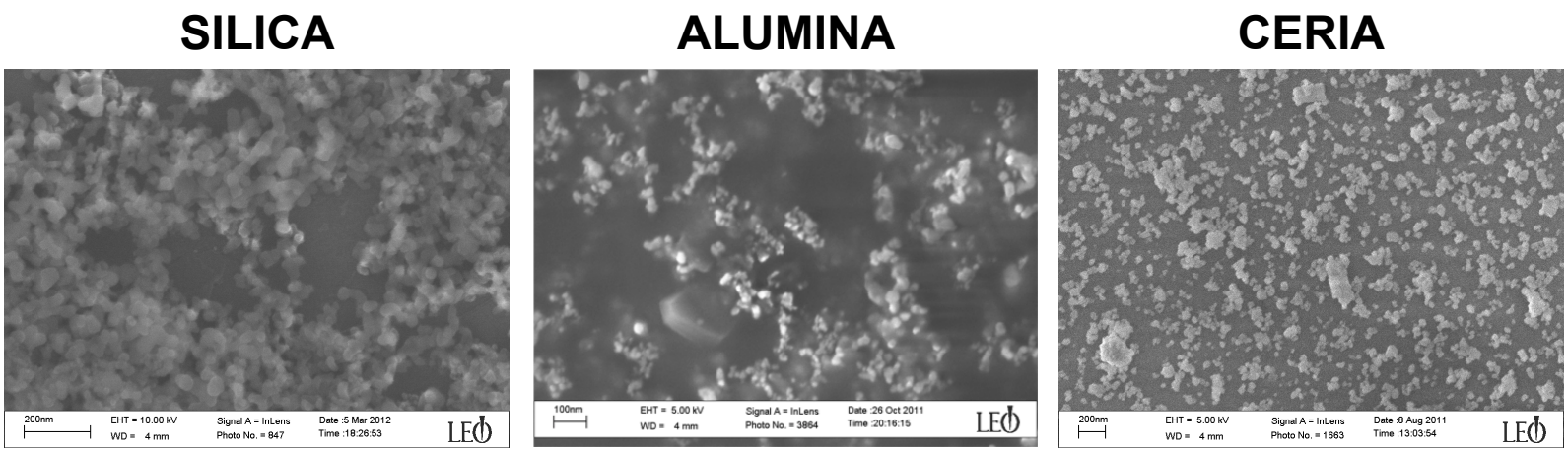

Metal oxide nanoparticles were characterized as described previously (Roth et al. 2015 [11]). SEM images show (left to right) silica, alumina, and ceria nanoparticles.

Figure S2: Metal oxide nanoparticles in areas of physiological relevance in lung tissue.

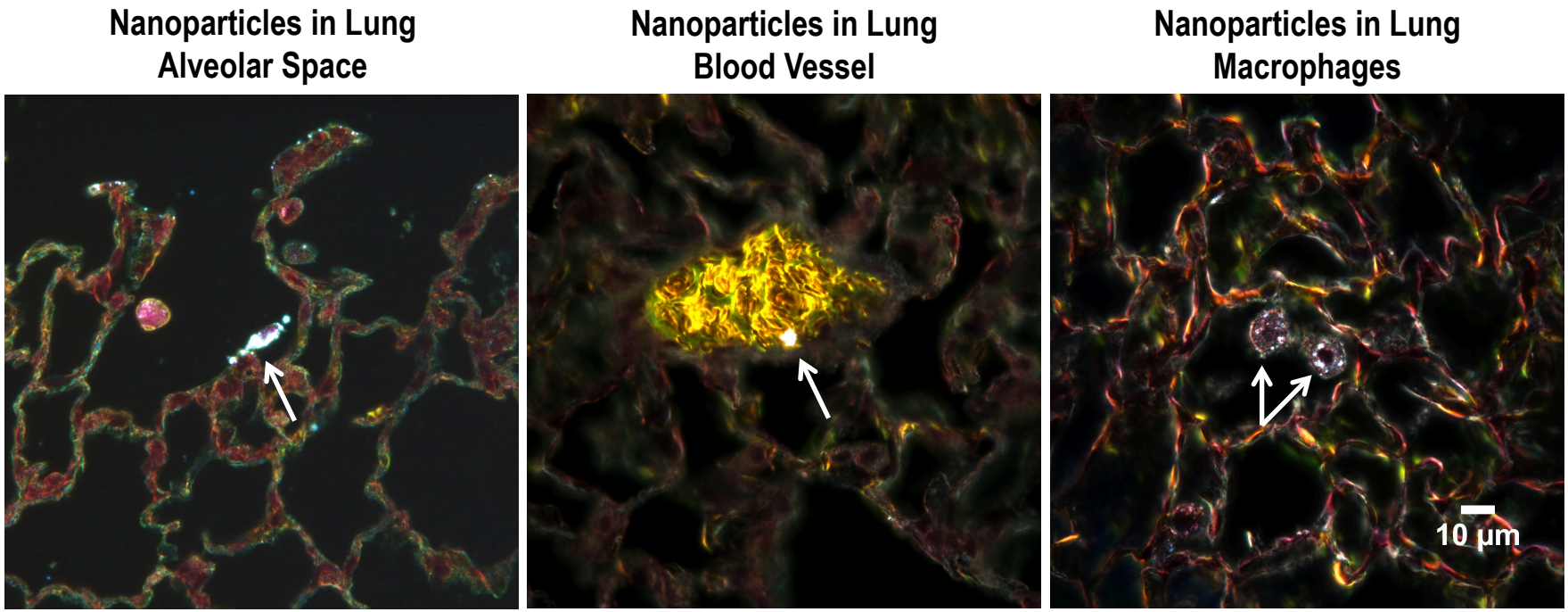

Darkfield images taken at 100x magnification show NPs in the lung tissue of rats exposed via inhalation to metal oxide NPs. Left: multiple NPs (arrow) are seen in the alveolar space in the lung of a silica-exposed rat; center: a cluster of NPs (arrow) is seen in a blood vessel amidst red blood cells in the lung tissue of an alumina-exposed rat; right: multiple NPs (arrows) are seen within two alveolar macrophages in lung tissue of a ceria-exposed rat.

Figure S3: Negative control tissues imaged with brightfield (BF) and enhanced darkfield microscopy (EDFM).

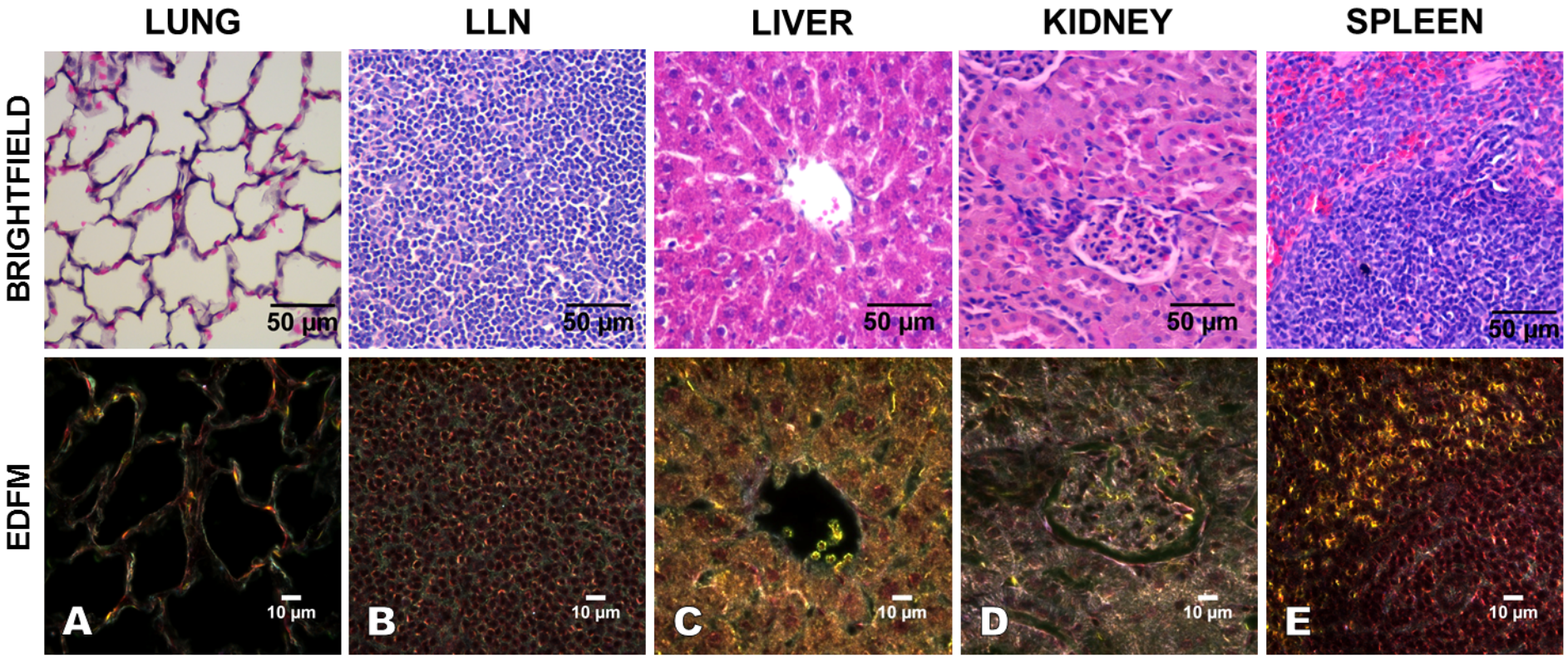

Negative control rats were exposed to filtered air for 6 hours and tissues were harvested at 24 hours post-exposure. Both BF (top row) and their respective EDFM images (bottom row) demonstrate the absence of high contrast elements or foreign NPs in these tissues and no signs of inflammation or physiological abnormalities. LLN, lung lymph node.

Figure S4: Biodistribution of nanoparticles (NPs) in organs of rats exposed via inhalation to silica NPs.

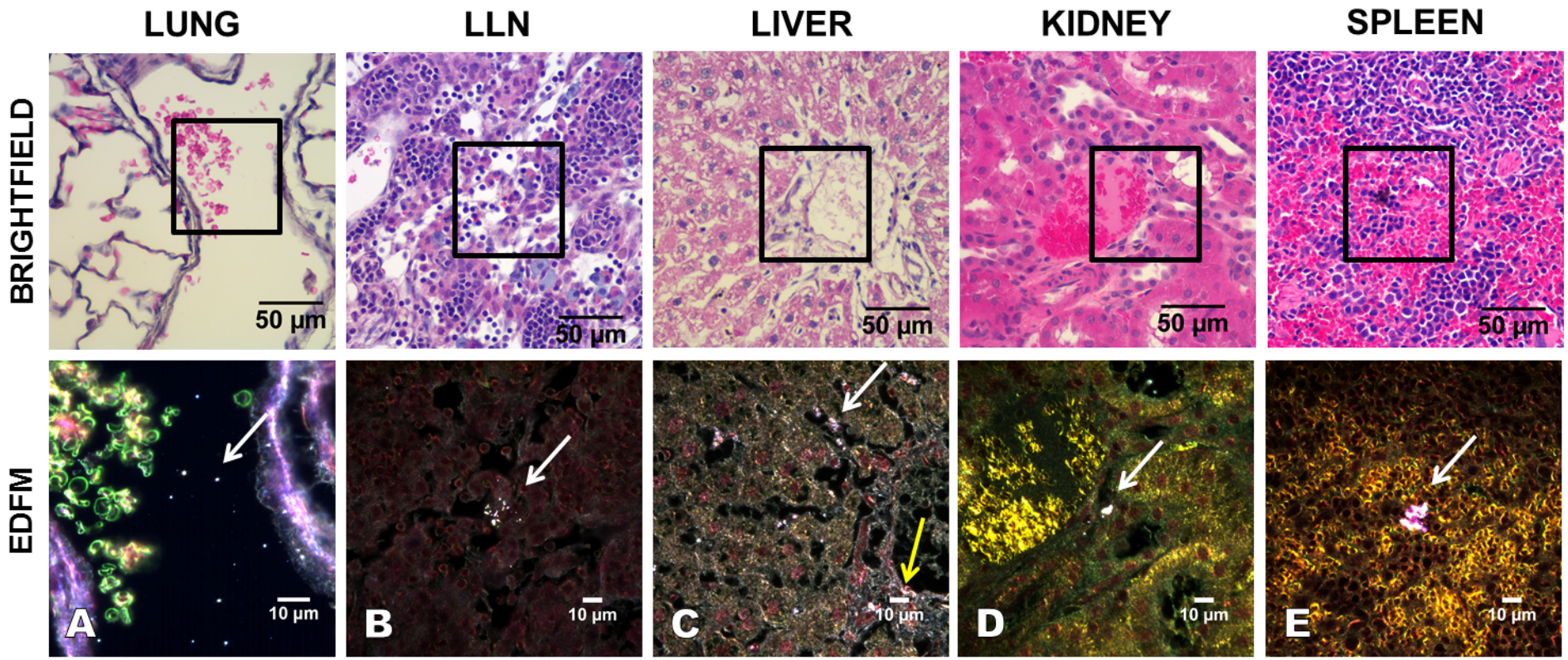

The top row shows BF images taken at 40x magnification, with their respective EDFM images at 100x magnification shown in the bottom row. From left to right: A) A blood vessel in the alveolar tissue of the lung contains multiple NPs (arrow) surrounded by red blood cells within the luminal space. This rat was exposed to a medium concentration (16.3 mg/m^3) of silica NP-containing slurry aerosol for 4 hours and sacrificed at 7 days post-exposure. B) An agglomeration of NPs (arrow) is seen among multiple white blood cells in the lymph node. This rat was exposed to a high concentration (34.0 mg/m^3) of silica slurry aerosol for 4 hours and sacrificed at 24 hours post-exposure. C) A portal triad in the liver with multiple NPs seen in both the connective tissue (yellow arrow) that supports its blood vessels and bile duct, and within the hepatic sinusoids (white arrow). This rat was exposed to a medium concentration (16.3 mg/m^3) of silica slurry aerosol for 4 hours and sacrificed at 24 hours post-exposure. D) A cluster of NPs (arrow) is seen in the kidney among renal tubules and adjacent to a blood vessel in the renal cortex. This rat was exposed to a high concentration (34.0 mg/m^3) of silica slurry aerosol for 4 hours and sacrificed at 24 hours post-exposure. E) Multiple agglomerated NPs (arrow) seen in the red pulp of the spleen. This rat was exposed to a high concentration (34.0 mg/m^3) of silica slurry aerosol for 4 hours, and sacrificed at 7 days post-exposure.

Figure S5: Biodistribution of NPs in organs of rats exposed via inhalation to alumina NPs.

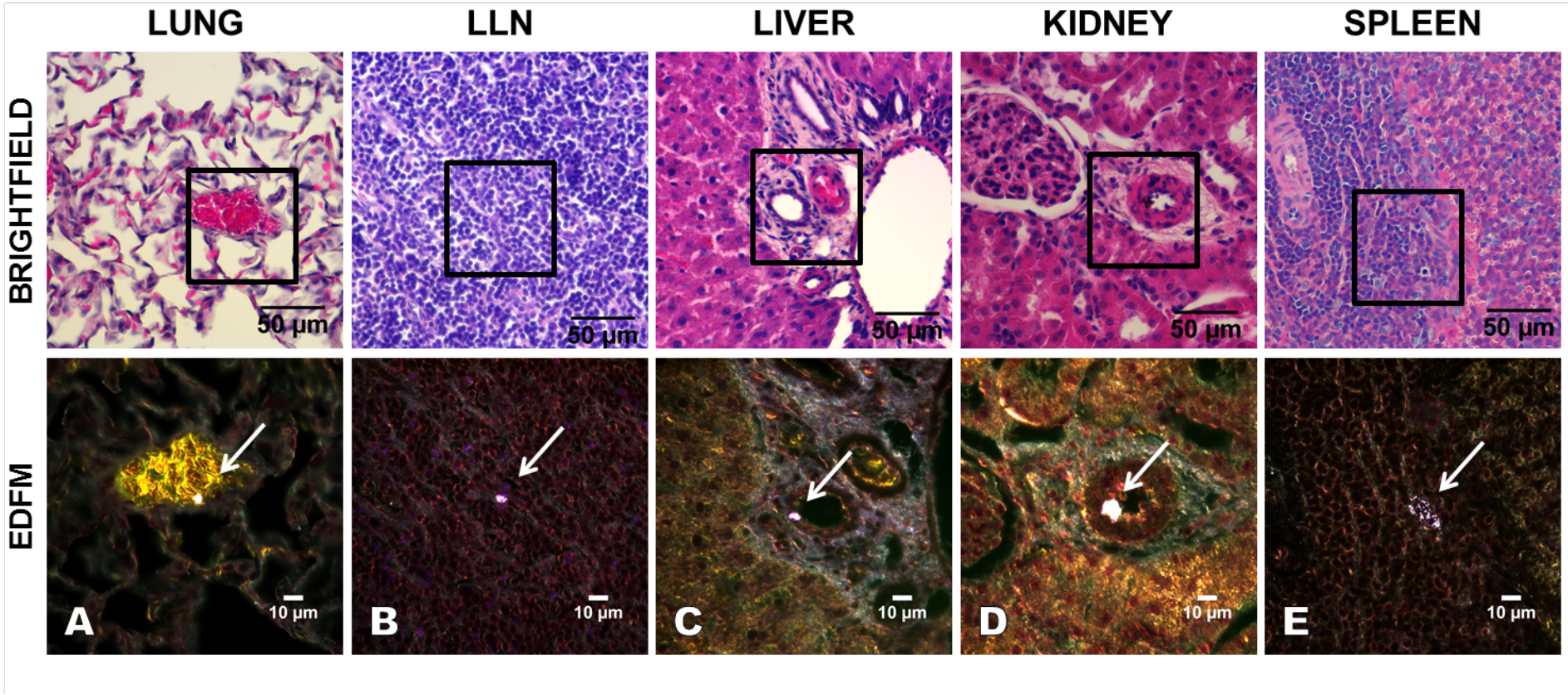

The top row shows BF images taken at 40x magnification, with their respective EDFM images at 100x magnification shown in the bottom row. From left to right: A) A blood vessel (shown as a cross-section filled with red blood cells) in the alveolar tissue of the lung shows a cluster of NPs (arrow) located inside the vessel lumen surrounded by red blood cells that appear pink in BF and yellow in DF. This rat was exposed to a low concentration (9.7 mg/m^3) of alumina NP-containing slurry aerosol for 4 hours, and sacrificed at 7 days post-exposure. B) A cluster of NPs (arrow) seen in a lung lymph node, surrounded by numerous white blood cells. This rat was exposed to a high concentration (20.9 mg/m^3) of alumina slurry for 6 hours, and sacrificed at 7 days post-exposure. C) A cluster of NPs (arrow) seen in the epithelial cells lining the bile duct of a portal triad in the liver. This rat was exposed to a high concentration (20.9 mg/m^3) of alumina slurry aerosol for 6 hours, and sacrificed at 24 hours post-exposure. D) A cluster of NPs (arrow) is seen in the endothelium lining a blood vessel in the kidney, adjacent to a glomerulus in the renal cortex. This rat was exposed to a low concentration (9.7 mg/m^3) of alumina slurry aerosol for 4 hours, and sacrificed at 24 hours post-exposure. E) Multiple NPs (arrow) are shown agglomerated in the white pulp of the spleen. This rat was exposed to a high concentration (20.9 mg/m^3) of alumina slurry aerosol for 6 hours, and sacrificed at 7 days post-exposure.

Figure S6: Biodistribution of NPs in organs of rats exposed via inhalation to ceria NPs.

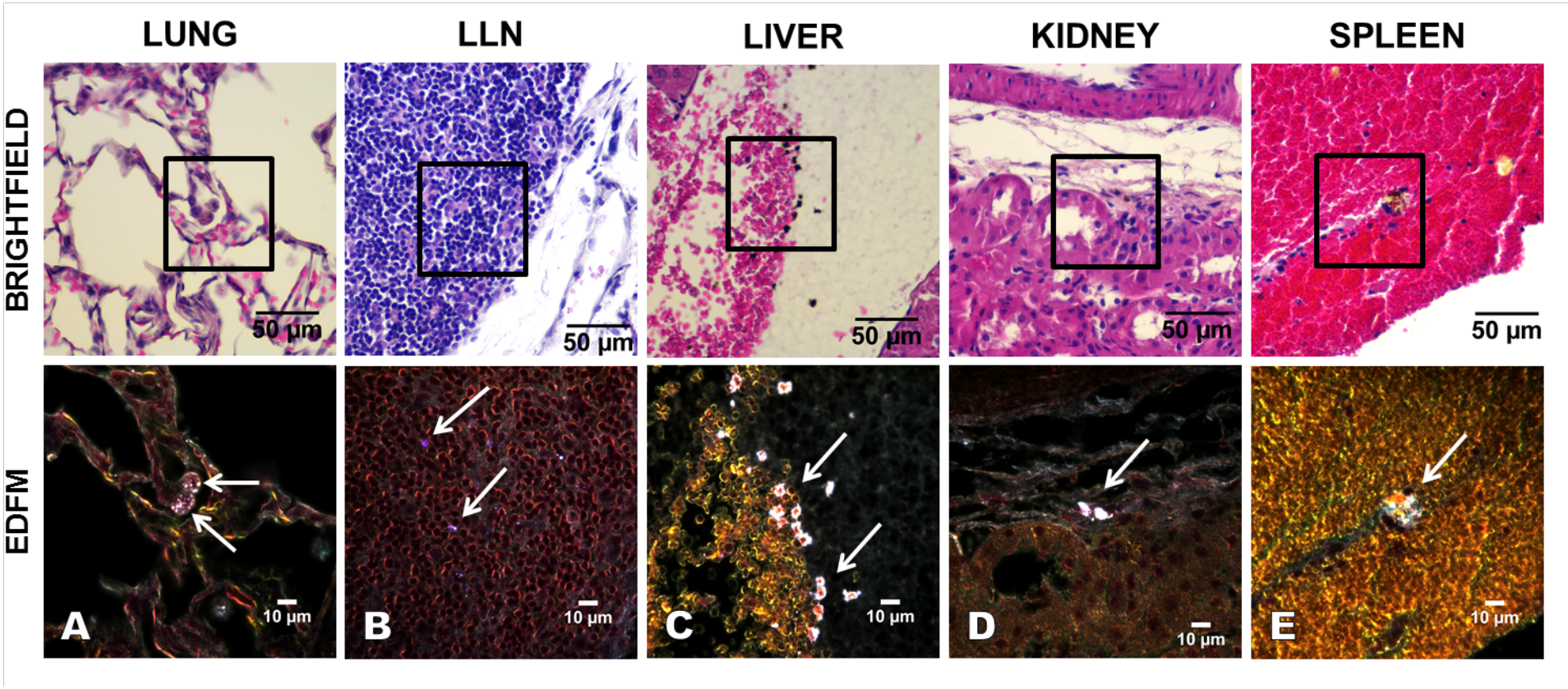

The top row shows BF images taken at 40x magnification, with their respective EDFM images at 100x magnification shown in the bottom row. From left to right, A) Multiple NPs (arrows) are seen within two alveolar macrophages in the alveolar space of the lung. This rat was exposed to a medium concentration (7.4 mg/m^3) of ceria NP-containing slurry aerosol for 4 hours, and sacrificed at 7 days post-exposure. B) Multiple NPs (arrows) are seen among the white blood cells in the lymph node. This rat was exposed to a high concentration (9.5 mg/m^3) of ceria slurry aerosol for 6 hours, and sacrificed at 24 hours post-exposure. C) A central vein in the liver shows a dilated lumen congested with red blood cells and multiple NPs (arrows). This rat was exposed to a medium concentration (7.4 mg/m^3) of ceria slurry aerosol for 4 hours, and sacrificed at 7 days post-exposure. D) Two clusters of NPs (arrow) are seen over the connective tissue adjacent to several tubules in the renal cortex. This rat was exposed to a high concentration (9.5 mg/m^3) of ceria slurry aerosol for 6 hours, and sacrificed at 24 hours post-exposure. E) Multiple agglomerated NPs (arrow) are shown in the red pulp of the spleen surrounded by numerous red blood cells. This rat was exposed to a low concentration (3.5 mg/m^3) of ceria slurry aerosol for 4 hours, and sacrificed at 24 hours post-exposure.